RSC Advances

RSC Advances

www.rsc.org/advances

ROYAL SOCIETY OF CHEMISTRY

www.rsc.org/advances

Journal Name

COMMUNICATION

Synthesis and Phase Transfer of Well-Defined BiVO4 Nanocrystals for Photocatalytic Water Splitting

Omer Yehezkeli,[1*] Albert Harguindey,[1] Dylan W. Domaille [1] Liangcan He,[1] Jennifer N. Cha[1,2*]

A method to synthesize BiVO4 nanoparticles and nanorods hydrothermally using sodium oleate as a capping ligand is presented. The BiVO4 nanocrystals possessed the expected blue shift in absorbance relative to bulk that occurs with scaling of particle size. Next, we transferred the BiVO4 nanoparticles from organic solvents to water using two different ligands. These particles were tested as water oxidation and dye reduction catalysts.

Extensive research has recently focused on discovering new solid state catalysts that can effectively split water using either externally biased[1-5] or unbiased electrodes.[6-17] While wide-band gap semiconductors like TiO_2[11] and WO_3[16, 18, 19] have been studied as photocatalysts for water-splitting, more recent efforts have turned to BiVO4 due to its bandgap of 2.4eV and ability to absorb in the visible.[1, 20] In the presence of electron scavengers such as $AgNO_3$ or $NaIO_3$, BiVO4 has also shown a strong ability to oxidize water and generate oxygen. Typically, BiVO4 has been grown by chemical vapor deposition (CVD)[21, 22] or chemical bath deposition (CBD)[23] on conductive surfaces, which has produced roughly structured, high surface area photoactive electrodes. In other work, BiVO4 photocatalysts have been obtained by reacting potassium vanadate powder with $Bi(NO_3)_3$ to yield nanoclusters that showed 9% quantum efficiency (at 450nm) as determined by the amount of oxygen generated under photoirradiation.[24] Amorphous shaped BiVO4–Ru/SrTiO3:Rh[9] or BiVO4/Graphene/SrTiO3[7] composites have also been synthesized to run complete water splitting to oxygen and hydrogen under visible light. Furthermore, Li and co-workers recently used micron sized M/MnO_x/BiVO4 and M/Co_3O_4/BiVO4 (M is a noble metal) composites to split water into oxygen and reduce methyl orange dye or $NaIO_3$.[25, 26] The co-catalysts in this case were selectively deposited by photoreduction or oxidation of Pt or MnOx nanocrystals respectively on different facets of the BiVO4 structures, which

led to better charge separation and lower back reactivities. More recently, co-catalysts like Co_3O_4, FeOOH and NiOOH were also electrodeposited on BiVO4 electrodes for improved water oxidation under illumination.[27] In order to improve catalytic performance, various BiVO4 architectures have also been doped with low amounts (~0.5-5%) of metals such as
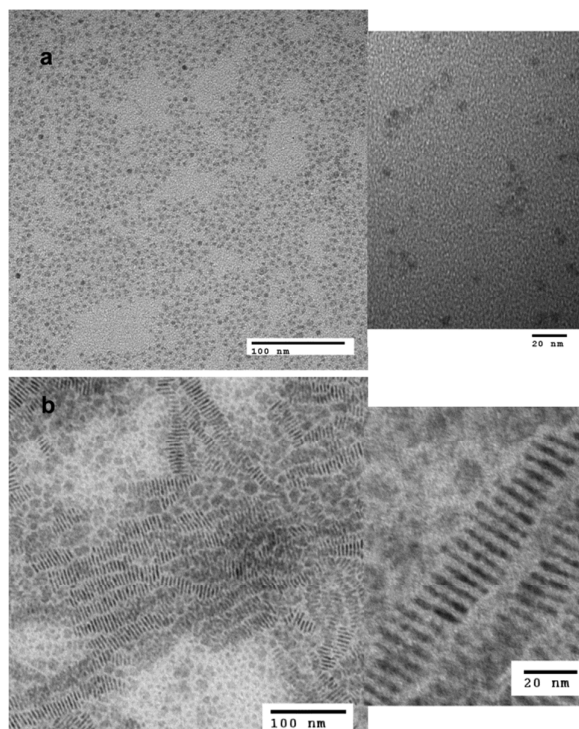
Fig 1. TEM images of the as prepared nano-sized BiVO4 (a) NPs (b)NRs

tungsten[28, 29], molybdenum[2] and phosphate[30] which allow better hole transport and enhanced water oxidation abilities. Recently, published work by Yang and coworkers showed an elegant and straightforward method to assemble BiVO4 wires with Rh-SrTiO3 to achieve water splitting.[31] Despite these

a. *Department of Chemical and Biological Engineering, University of Colorado, Boulder, USA*
b. *Materials Science and Engineering Program, University of Colorado, Boulder, USA*

successes in producing photoactive $BiVO_4$ however, the synthesis of well-defined nanostructures of $BiVO_4$ with control over both size and shape has remained challenging. Although a recent report showed successful hydrogen generation by nanosized $BiVO_4$ in water presumably due to the change in energy levels as compared to bulk, the size and shape of the particles were less defined and the photocatalytic studies were run using surfactant coated particles which is known to impede electron and hole transfer.[32] Other reports showed well defined $BiVO_4$ NRs[33] or tubes[34], but the sizes exceed 100nm. Because of this, methods to obtain monodisperse and well-defined $BiVO_4$ nanoparticles (NPs) and nanorods (NRs) were first pursued. As expected with particle scaling, a distinct blue shift in absorbance was observed from bulk indicating an increase in band gap energy. Next ligand exchange techniques that removed the large hydrocarbons from the particle surfaces and enabled their effective transfer to aqueous solutions were developed. Despite their blue shift in absorbance, when testing the photocatalytic performance of the $BiVO_4$ NPs and NRs, a significant improvement in water oxidation as compared to micron-sized $BiVO_4$ in the presence of sodium persulfate as an electron acceptor was observed. Finally, in the absence of any sacrificial donors it was found that the $BiVO_4$ could reduce the dye molecule dichlorophenolindophenol (DCPIP) upon photoillumination in an oxygen-free environment.

In a typical synthesis, 1g of $Bi(NO_3)_3$ was dissolved in 100ml of DI water and stirred in a 250ml reaction vessel for 10min at room temperature. The temperature was next raised to 60^0C at which point 1.825 g of sodium oleate was added. The temperature was then raised to 80^0C followed by the dropwise addition of 250 mg of NH_4VO_3 dissolved in 50 ml of water. The reaction vessel was then sealed and the solution was continuously stirred during which the solution changed slowly from a milky white color to a yellow slurry. At different time points between 3 and 20 hours, the reactions were quenched by removing the flasks from heat and the products were collected by precipitation in water and centrifugation. The solids were then dissolved in toluene to obtain clear yellow-orange solutionssolutions, while the precipitated material (waste) was discarded. As shown in Fig 1a, using these synthesis procedures we were able to obtain after 3hrs ~4.5nm spherical nanoparticles that were well dispersed and stable in organic solvents (Fig S1a). X-ray diffraction (XRD) analyses of the as-synthesized nanoparticles showed that they possessed the tetragonal form of $BiVO_4$ (Fig S2a). After 20 hours of synthesis we found that the spherical morphologies transitioned to nanorods (NRs) that were 4.7 nm in diameter and ~ 20 nm in length (Fig 1b, Fig S1b). The XRD measurement showed that like the NPs, the NRs also adopted the tetragonal form of $BiVO_4$ a mixed form35, 36 of tetragonal and monoclinic which could be attributed to the presence of other nanostructures (mainly NPs) in the NRs solutions, (Fig S2b). UV/Vis absorbance measurements showed a distinct blue shift in the absorbance onset which increased as we moved from the NR samples to the NPs (Fig S3). Using the measured absorbance values, the band gaps of the NPs and NRs were

determined to be 3.35 eV and 2.91 eV respectively. It should be noted that the NRs samples did contain a small portion of NPs. Furthermore by using different reaction times such as 6 or 12 hrs we obtained products that consisted of NPs largely with small amounts of NRs. We also examined the use of different pressure vessels for the reactions, which although led to the use of shorter reaction times to produce $BiVO_4$ NRs, yielded primarily NR and NP mixtures.

In order to test the photocatalytic activity of the as-synthesized $BiVO_4$ NPs and NRs, methods to transfer the particles from toluene to water first needed to be developed. Although previous reports demonstrated the use of $BiVO_4$ particles for water oxidation, these were typically run using either a suspension of surfactant coated $BiVO_4$ nanoparticles or larger structures that were ligands free and therefore tended to precipitate out. After trying a number of small molecule ligands, we found we could achieve the best phase transfer of the as-synthesized $BiVO_4$ NPs and NRs from toluene or chloroform to water with meso 2,3-dimercaptosuccinic acid (DMSA). For this, the as-synthesized oleic-capped $BiVO_4$ NPs
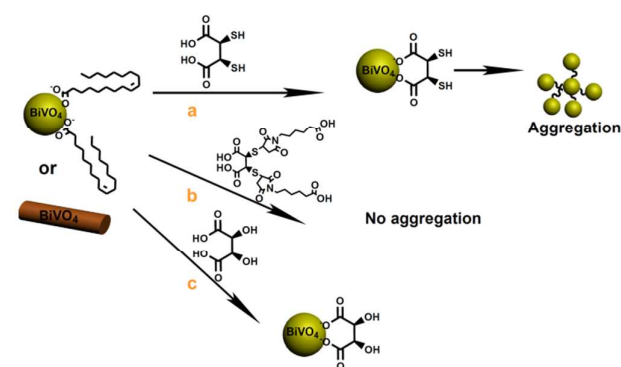
Fig 2. Schematic illustration of the different ligand exchange routes (a) the addition of DMSA to the BiVO4-oleate leads to water soluble NPs/NRs which start to aggregate after a few hours (b) Addition of DMSA-EMCA led to water soluble BiVO4 NPs/NRs with no aggregation (c) Addition of tartaric acid led to water soluble BiVO4 NPs/NRs with no aggregation.

and NRs were first mixed with DMSA in toluene for 10min followed by the addition of DI water and mixing. After stirring the solution for a few hours the $BiVO_4$ NPs and NRs started to transfer to the aqueous phase (Fig 2a). The DMSA molecule is thought to work through the carboxylic acid groups binding to the $BiVO_4$ surface while leaving the thiols free to impart water solubility. Fig 3 presents images of the ligand exchange process before, during and after the ligand exchange to the water phase. Greater evidence that the thiol groups of the DMSA are
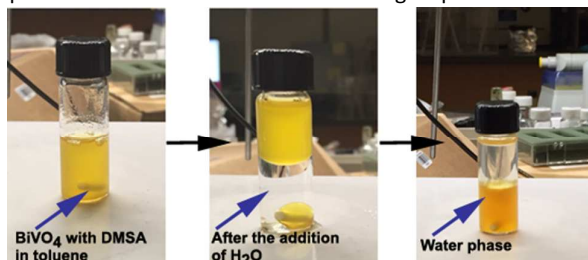
exposed from the NP surfaces was shown when the NPs started to aggregate a few hours after being transferred to the aqueous phase presumably due to thiol

Fig 3. The ligand exchange process (left), a mixture of the $BiVO_4$ with DMSA in toluene (middle), after the addition of water (right), after mixing the two solutions overnight.

Greater evidence that the thiol groups of the DMSA are exposed from the NP surfaces was shown when the NPs started to aggregate a few hours after being transferred to the aqueous phase presumably due to thiol oxidation (Fig S4). In order to circumvent this, we tried two different methods- (i)

react DMSA with maleimidocaproic acid (EMCA) prior to ligand exchange to prevent thiol oxidation (Fig 2, route b) or (ii) react the NPs or NRs with tartaric acid (Fig 2, route c). From these studies, we found that by either capping the free thiols on DMSA and simply replacing the thiols with alcohol groups could effectively prevent nanoparticle aggregation (Fig S5). The ligand exchange process was also observed to occur more quickly with the DMSA-EMCA molecules as compared to tartaric acid (TA) which required an overnight reaction for complete phase transfer.
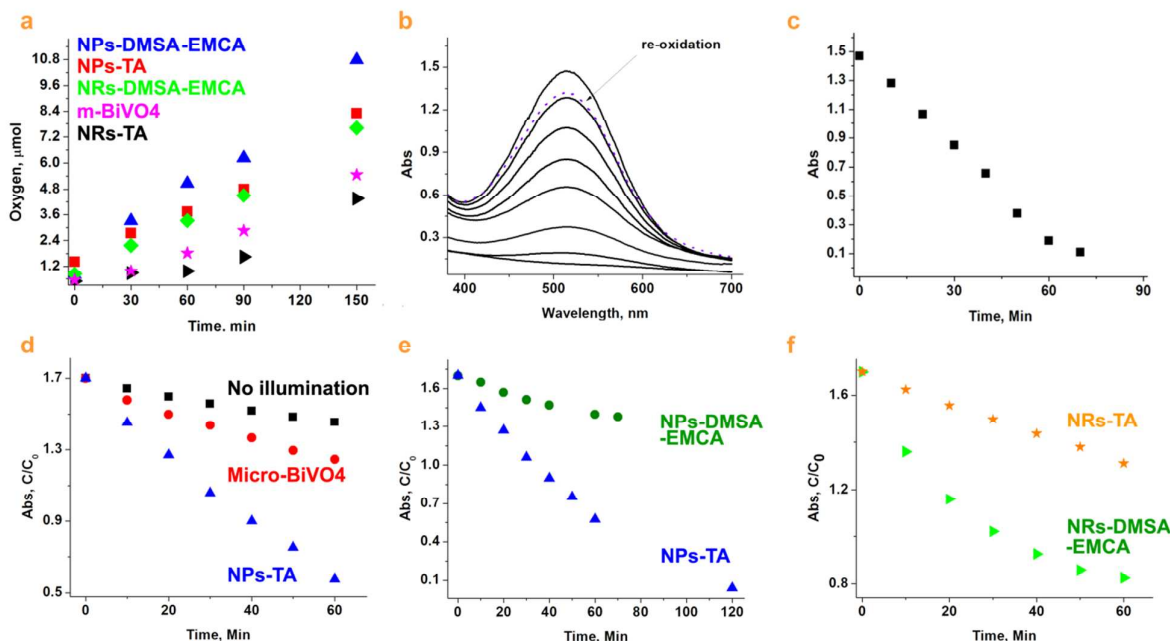
Fig 4. Photocatalytic activity of the nano- $BiVO_4$: (a) oxygen amount generated by the NPs or NRs coated with either TA or DMSA-EMCA b) Photocatalytic activity of the TA conjugated $BiVO_4$ NPs ,as determined by UV/Vis. The samples were purged first for 20 minutes with nitrogen and the DCPIP photoreduction was measured at 525 nm. (c) The color depletion rate of (b). The DCPIP was reoxidized by adding persulfate to the cuvette, Fig 4b, dashed line. (d) Photocatalytic activity of the TA coated NPs (light on: blue triangles; light off: black squares) compared to the photoilluminated micron-sized $BiVO_4$ (red circles). (e) DCPIP photoreduction activity of the TA (triangles) and DMSA-EMCA (circles) conjugated NPs (f) DCPIP photoreduction activity of the DMSA-EMCA NRs (triangles) compared to the TA coated NRs (stars). For the photoreduction studies, all of the measurements were performed using 495 μl water, 100 μl of the $BiVO_4$ catalyst (1 mg/ml) and 5 μl of DCPIP (1 mg/ml). The cuvette was blanked before the addition of the DCPIP and then sealed and purged for 20min with N_2 and photoilluminated for 1-2 hrs under 1 sun. The absorbance was monitored by UV/Vis at 10 minute intervals

It should be noted that although after several weeks slight aggregation was seen in both the DMSA-EMCA and TA conjugated nanoparticles, this was minute compared to the DMSA only treated samples (Fig S6). Furthermore, the capping ligands used were found to influence the optical properties of the particles where the DMSA-EMCA conjugated nanocrystals absorbed at longer wavelengths as compared to the TA bound $BiVO_4$ (Fig S7).

After the successful phase transfer into water, the $BiVO_4$ NPs and NRs were next tested for water oxidation. For this,

sodium persulfate was added as a sacrificial electron acceptor and the samples were sealed and bubbled with argon to remove oxygen from the cuvette. The degassed samples were then placed under a solar simulator and the oxygen generated was monitored by a gas chromatogram (GC) equipped with a 5A column and TCD detector. Fig 4a presents the oxygen produced from $BiVO_4$ NPs and NRs capped with the TA or DMSA-EMCA. The largest amount of oxygen generated per particle was found to occur from the DMSA-EMCA conjugated NPs (blue triangles) with slightly less activity from the TA

coated NPs (red squares). While the DMSA-EMCA conjugated NRs (green diamonds) showed comparable data to the TA bound NPs, much lower activities were seen from the TA coated NRs (black triangles). Overall the higher water oxidation activities observed with the NPs over the NRs can be attributed to the larger number of moles of NPs used as compared to NRs. Since the catalytic studies were performed per mass of $BiVO_4$, it is expected that the smaller spherical NPs would yield a greater number of particles used than that for the larger NRs. In comparing however the nanoscale $BiVO_4$ particles to micron sized $BiVO_4$ synthesized using previously published procedures[25] (Fig S8), significantly higher water oxidation was observed from the NPs and the DMSA-EMCA bound NRs. It must be noted here that this significant gain in catalysis was obtained despite the $BiVO_4$ nanostructures absorbing primarily in the UV portion of the solar spectrum (Fig S9).

In addition to water oxidation, the photoreduction properties of the $BiVO_4$ NPs and NRs were studied by using the dye molecule 2,6-Dichlorophenol Indophenol (DCPIP). For this, the particles were dispersed in water with DCPIP in a sealed cuvette, purged with nitrogen for 20 minutes to remove any free oxygen and then irradiated under 1 sun. In the absence of any sacrificial donors, the reduction of the dye was determined by measuring a decrease in absorbance at 525nm. As shown in Fig 4b, in the presence of the tartaric acid (TA) coated $BiVO_4$ NPs, a distinct decrease in absorbance was observed and the solution became optically clear after 70minutes (Fig 4c). In order to verify that the dye was becoming reduced as opposed to being photodegraded, after photoillumination, sodium persulfate ($Na_2S_2O_8$) was added as an oxidant to successfully regenerate the original state of the dye molecule (Fig 4b, dashed line). Due to the larger band gap of the $BiVO_4$ nanostructures, higher photoreduction activity was observed from the $BiVO_4$ NPs (Fig 4d, triangles) as compared to the micron-sized $BiVO_4$ (Fig 4d, circles). We also compared the effect of ligands on the $BiVO_4$ nanocrystals on photoreduction as a function of particle morphology. As shown in Fig 4e and 4f, while the TA conjugated NPs showed significantly better activity as compared to the DMSA-EMCA coated NPs, this phenomena was reversed with the $BiVO_4$ NRs demonstrating that the ligands bound can have a direct effect on catalysis. While the effect of ligands on the nanoparticles was also seen with the water oxidation studies due to changes in nanocrystal absorption (Fig 4a), the lowering in DCPIP photoreduction with the DMSA-EMCA coated NPs as compared with the TA conjugated NPs appeared counterintuitive. One possible explanation of this is that the combined use of DMSA and EMCA leads to an organic coating that possesses a much greater overall volume as compared to TA making it difficult for molecules such as DCPIP to reach the surface of the small spherical $BiVO_4$ NPs. Therefore, while a small molecule like water may not have a difficult time to reach the small spherical NP surface, a much larger compound such as DCPIP might. In the case of the $BiVO_4$ NRs however, since there is much less of an effect of surface crowding by any ligands attached, the observed widening in absorbance of the DMSA-EMCA coated NRs dominated to lead to an overall

increase in photoreduction over that of with the DMSA-EMCA coated NRs was most likely due to the ligands causing a widening in the NR absorbance towards the visible that was not seen with the TA coated NRs (Fig S7). While it is possible that the negative charge of the acid groups on EMCA could also influence catalytic activity, as our experiments were run at pH 5, any charge effect should be minimized.

Conclusions

In conclusion, we have demonstrated here a new method to synthesize well-defined $BiVO_4$ NPs and NRs that are monodisperse in size and shape. In addition, we showed for the first time two different strategies to transfer the as-synthesized $BiVO_4$ particles from organic solvent to water through ligand exchange by using DMSA and EMCA or tartaric acid. These NPs and NRs were further tested for both water oxidation and dye reduction upon photoillumination in the absence of any sacrificial donors and in both cases, showed significantly higher catalytic activity as compared to micron-sized $BiVO_4$ particles. These gains in activity were observed despite the $BiVO_4$ nanocrystals absorbing primarily in the UV portion of the solar spectrum, illustrating the importance of having high surface area materials for catalysis. Lastly, we also showed that the ligands on the particles could have a direct influence on their optical properties and photocatalytic performance which was also dependent on nanocrystal size and morphology. Future studies will investigate the use of doping the $BiVO_4$ nanostructures to shift the absorbance into the visible regime of the solar spectrum and thereby further increase their photocatalytic performance.

Notes and references

1   Q. Jia, K. Iwashina and A. Kudo, Proc. Natl. Acad. Sci., 2012, 109, 11564–11569.
2   J. A. Seabold, K. Zhu and N. R. Neale, Phys. Chem. Chem. Phys., 2013, 16, 1121–1131.
3   M. W. Kanan and D. G. Nocera, Science, 2008, 321, 1072–1075.
4   R. Costi, E. R. Young, V. Bulović and D. G. Nocera, ACS Appl. Mater. Interfaces, 2013, 5, 2364–2367.
5   O. Yehezkeli, D. R. B. de Oliveira and J. N. Cha, Small, 2014, 6, 667.
6   K. Maeda and K. Domen, Angew. Chem. Int. Ed., 2012, 51, 9865–9869.
7   A. Iwase, Y. H. Ng, Y. Ishiguro, A. Kudo and R. Amal, J. Am. Chem. Soc., 2011, 133, 11054–11057.

Journal Name COMMUNICATION

8   F. F. Abdi, L. Han, A. H. M. Smets, M. Zeman, B. Dam and R. van de Krol, Nat. Commun., 2013, 4.

9   Q. Jia, A. Iwase and A. Kudo, Chem. Sci., 2014, 5, 1513–1519.

10 K. Kalyanasundaram, E. Borgarello and M. Grätzel, Helv. Chim. Acta, 1981, 64, 362–366.

11 S. U. M. Khan, M. Al-Shahry and W. B. Ingler, Science, 2002, 297, 2243–2245.

12 L. Liao, Q. Zhang, Z. Su, Z. Zhao, Y. Wang, Y. Li, X. Lu, D. Wei, G. Feng, Q. Yu, X. Cai, J. Zhao, Z. Ren, H. Fang, F. Robles-Hernandez, S. Baldelli and J. Bao, Nat. Nanotechnol., 2014, 9, 69–73.

13 G. Liu, J. Shi, F. Zhang, Z. Chen, J. Han, C. Ding, S. Chen, Z. Wang, H. Han and C. Li, Angew. Chem. Int. Ed., 2014, 53, 7295–7299.

14 K. Maeda, ACS Catal., 2013, 3, 1486–1503.

15 K. Maeda, K. Teramura, T. Takata, M. Hara, N. Saito, K. Toda, Y. Inoue, H. Kobayashi and K. Domen, J. Phys. Chem. B, 2005, 109, 20504–20510.

16 K. Maeda, A. Xiong, T. Yoshinaga, T. Ikeda, N. Sakamoto, T. Hisatomi, M. Takashima, D. Lu, M. Kanehara, T. Setoyama, T. Teranishi and K. Domen, Angew. Chem. Int. Ed., 2010, 49, 4096–4099.

17 F. Zhang, A. Yamakata, K. Maeda, Y. Moriya, T. Takata, J. Kubota, K. Teshima, S. Oishi and K. Domen, J. Am. Chem. Soc., 2012, 134, 8348–8351.

18 R. Abe, T. Takata, H. Sugihara and K. Domen, Chem. Commun., 2005, 3829–3831.

19 J. Su, X. Feng, J. D. Sloppy, L. Guo and C. A. Grimes, Nano Lett., 2011, 11, 203–208.

20 W. Luo, Z. Yang, Z. Li, J. Zhang, J. Liu, Z. Zhao, Z. Wang, S. Yan, T. Yu and Z. Zou, Energy Environ. Sci., 2011, 4, 4046–4051.

21 E. Alarcón-Lladó, L. Chen, M. Hettick, N. Mashouf, Y. Lin, A. Javey and J. W. Ager, Phys. Chem. Chem. Phys., 2013, 16, 1651–1657.

22 W. Luo, Z. Wang, L. Wan, Z. Li, T. Yu and Z. Zou, J. Phys. Appl. Phys., 2010, 43, 405402.

23 J. Su, L. Guo, N. Bao and C. A. Grimes, Nano Lett., 2011, 11, 1928–1933.

24 A. Kudo, K. Omori and H. Kato, J. Am. Chem. Soc., 1999, 121, 11459–11467.

25 R. Li, F. Zhang, D. Wang, J. Yang, M. Li, J. Zhu, X. Zhou, H. Han and C. Li, Nat. Commun., 2013, 4, 1432.

26 R. Li, H. Han, F. Zhang, D. Wang and C. Li, Energy Environ. Sci., 2014, 7, 1369–1376.

27 T. W. Kim and K.-S. Choi, Science, 2014, 343, 990–994.

28 H. S. Park, H. C. Lee, K. C. Leonard, G. Liu and A. J. Bard, ChemPhysChem, 2013, 14, 2277–2287.

29 D. K. Zhong, S. Choi and D. R. Gamelin, J. Am. Chem. Soc., 2011, 133, 18370–18377.

30 W. J. Jo, J.-W. Jang, K. Kong, H. J. Kang, J. Y. Kim, H. Jun, K. P. S. Parmar and J. S. Lee, Angew. Chem. Int. Ed., 2012, 51, 3147–3151.

31 B. Liu, C.-H. Wu, J. Miao, P. Yang, *ACS Nano.* 2014, **8**, 11739.

32 S. Sun, W. Wang, D. Li, L. Zhang and D. Jiang, ACS Catal., 2014, 4, 3498–3503.

33   Y. Zhang, Y. Guo, H. Duan, H. Li, C. Sun and H. Liu, Phys. Chem. Chem. Phys., 2014, 16, 24519-24526.

34 Y. Sun, Y. Xie, C. Wu, S. Zhang, and S. Jiang, Nano Res. 2010, 3, 620–631

35 D. Ke, T.Peng , L. Ma, P. Cai and K. Dai Inorg. Chem., 2009, 48, 4685–4691

36 H. Fan, T. Jiang, H. Li, D. Wang, L. Wang, J. Zhai, D. He, P. Wang, and T. Xie J. Phys. Chem. C, 2012, 116, 2425–2430